

Zero-Shot Function Encoder-Based Differentiable Predictive Control

Hassan Iqbal

Xingjian Li

Tyler Ingebrand

Adam Thorpe

Krishna Kumar

Ufuk Topcu

The University of Texas at Austin, 78712, TX, USA

HASSAN.IQBAL@UTEXAS.EDU

XINGJIAN.LI@AUSTIN.UTEXAS.EDU

TYLERINGEBRAND@UTEXAS.EDU

ADAM.THORPE@AUSTIN.UTEXAS.EDU

KRISHNAK@UTEXAS.EDU

UTOPCU@UTEXAS.EDU

Ján Drgoňa

Johns Hopkins University, Baltimore, 21218, MD, USA

JDRGONA1@JH.EDU

Abstract

We introduce a differentiable framework for zero-shot adaptive control over parametric families of nonlinear dynamical systems. Our approach integrates a function encoder-based neural ODE (FE-NODE) for modeling system dynamics with differentiable predictive control (DPC) for offline self-supervised learning of explicit control policies. The FE-NODE captures nonlinear behaviors in state transitions and enables zero-shot adaptation to new systems without retraining. While the DPC efficiently learns control policies across system parameterizations, thus eliminating costly online optimization common in classical model predictive control. We demonstrate the efficiency, accuracy, and online adaptability of the proposed method across a range of nonlinear systems with varying parametric scenarios, highlighting its potential as a general-purpose tool for fast zero-shot adaptive control.

Keywords: differentiable predictive control, function encoder, neural ordinary differential equations, system identification, learning to control

1. Introduction

Learning-based control methods rely on fixed models or predefined datasets of observations to train, which limits their ability to generalize when system parameters or environmental conditions change online. Systems such as aircraft flying through variable wind fields (Beliaev et al., 2023) or delivery drones carrying shifting payloads (Palunko and Fierro, 2011) require controllers that can adjust to new dynamics in real-time, without retraining or reoptimization. However, real-time adaptation remains challenging because most optimization-based and learning-based controllers depend on expensive, repeated online updates or gradient-based policy refinement. These computations introduce significant computational overhead, making them unsuitable for fast or safety-critical operation. Achieving zero-shot control, in which a learned policy adapts to new dynamics without additional online optimization, requires closed-loop control policies that can adjust instantaneously to variations in the underlying system dynamics.

We present a method for zero-shot control that combines function encoders (FE) with differentiable predictive control (DPC) to achieve adaptive closed-loop policies without costly online optimization. Parametric differentiable predictive control provides a gradient-based approach to optimal control via end-to-end learning of feedback control policies through backpropagation. However, its viability hinges on the underlying parametric dynamical system being fully known and differentiable, a condition often unmet in real-world problems due to noise, system degradation, and other

uncertainties (Le Lidec et al., 2024; List et al., 2025). To overcome this limitation, we condition the learned DPC control policy on a compact learned representation of the underlying system using function encoders (Ingebrand et al., 2024a). Function encoders represent the dynamics as a linear combination of learned neural ODE basis functions, thereby enabling zero-shot modeling by efficiently computing the corresponding basis coefficients online from limited system measurements. Conditioning the DPC policy on the function encoder coefficients allows the controller to adjust instantaneously to new and unseen dynamics at runtime.

Related Work. Model predictive control (MPC) remains the industry standard for controlling multi-input, multi-output constrained systems (Borrelli et al., 2017; Rawlings et al., 2020; Samad et al., 2020; Schwenzer et al., 2021). MPC excels in accuracy and reliability for a wide range of problems through receding-horizon optimization, but as control systems become increasingly complex, solving the associated online optimization problems repeatedly with accurate models can become prohibitively expensive. This has inspired work that focuses on hardware acceleration and algorithm optimization, such as (Houska et al., 2011; Verschueren et al., 2021; Adabag et al., 2024; Zanelli et al., 2020; Frison and Diehl, 2020; Wu and Bemporad, 2023). Requiring an accurate and fully differentiable dynamics model is often another bottleneck for MPC solvers. Integrating system identification or uncertainty quantification with classic MPC solvers (Koller et al., 2018; Fasel et al., 2021; Martinsen et al., 2020; Al Seyab and Cao, 2008) can serve as a solution; however, it also introduces additional cost and error accumulation, limiting practicality.

While accurate, the high online cost of MPC solvers limits their use in many real-time control applications. Learning-based and data-driven approaches (Hewing et al., 2020; Jiang et al., 2020; Berberich et al., 2021) have emerged as an effective alternative. These methods amortize control computation through offline training, enabling real-time deployment. Existing approaches can be broadly categorized into supervised learning-based approximate MPC, such as (Hertneck et al., 2018; Chen et al., 2018b; Karg and Lucia, 2020; Pin et al., 2013; Li et al., 2025a), which learn policies directly from trajectories or expert demonstrations, and self-supervised methods (Jin et al., 2020; Drgoňa et al., 2022; Onken et al., 2022; Drgoňa et al., 2024), which rely on known differentiable dynamics and objectives for policy optimization.

Function encoders (Ingebrand et al., 2025; Low et al., 2025) provide a structured and principled framework for neural network-based function space approximation, with prominent applications in reinforcement learning (Ingebrand et al., 2024b) and control (Ward et al., 2025; Li et al., 2025b). In this work, we focus on system identification (Ingebrand et al., 2024a), which extends from prior classical (Isermann and Münchhof, 2011; Pintelon and Schoukens, 2012) and learning-based methods such as NODE (Chen et al., 2018a; Rahman et al., 2022), SINDy (Brunton et al., 2016), Koopman operator (Korda and Mezić, 2018; Klus et al., 2020) and more. Function encoders offer retraining-free adaptability to different dynamics, an ability that existing methods often lack.

Contributions. We propose a framework for zero-shot adaptive control that combines function-encoder-based system identification with differentiable predictive control, as illustrated in Figure 1. Our main contributions are: 1) *Zero-shot control via function-encoder representation*. We develop a differentiable control architecture in which system dynamics are represented using a compact FENODE basis and identified online through low-cost coefficient inference. A parametric DPC policy is trained offline over this learned dynamics space, enabling instantaneous online adaptation to previously unseen dynamics without retraining or reoptimization. 2) *Scalable performance across nonlinear and high-dimensional benchmarks*. We demonstrate the proposed method on a range of

nonlinear control tasks, including the Van der Pol oscillator, two-tank level regulation, a stiff glycolytic oscillator, and a 12D quadrotor model. Across these settings, the learned policies maintain closed-loop stability under abrupt dynamics changes and achieve orders-of-magnitude faster inference compared to online MPC, while retaining competitive control performance. 3) *Open-source implementation*¹. We release all code, models, and training pipelines to enable reproducibility.

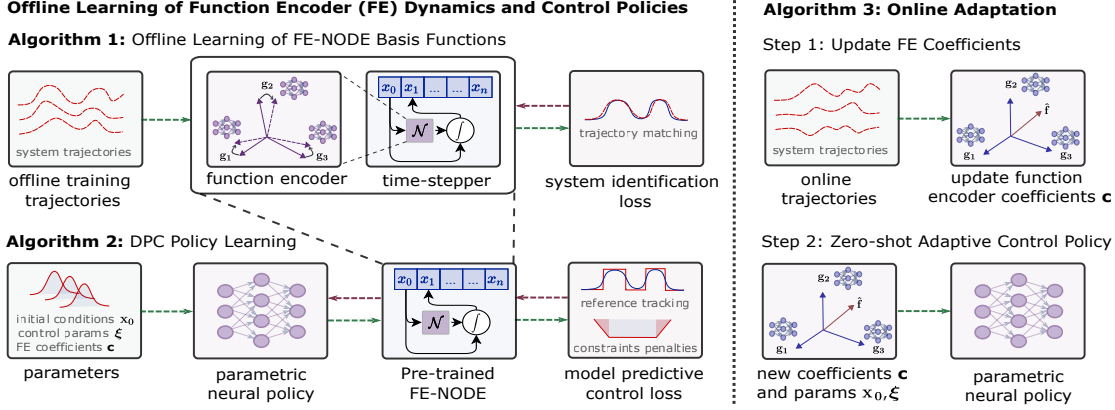


Figure 1: Conceptual diagram of the proposed Function-Encoder Differentiable Predictive Control.

2. Problem Formulation

We consider a general class of parametric optimal control problems (pOCP) that take the following continuous-time form

$$\min_{\pi \in \Pi} \mathbb{E}_{\mathbf{x}_0 \sim P_{\mathbf{x}_0}, \xi \sim P_{\xi}, \nu \sim P_{\nu}} \left(\int_0^T \ell(\mathbf{x}(t), \mathbf{u}(t); \xi) dt + p_T(\mathbf{x}(T)) \right) \quad (1a)$$

$$\text{s.t. } \frac{d\mathbf{x}(t)}{dt} = \mathbf{f}(\mathbf{x}(t), \pi(\mathbf{x}(t); \xi, \nu); \nu), \quad (1b)$$

$$h(\mathbf{x}(t); \xi) \leq 0, \quad g(\mathbf{u}(t); \xi) \leq 0, \quad (1c)$$

where ξ is a set of parameters that determine constraints and objective functions for the given problem, T is the prediction horizon, h and g are continuously differentiable state and control constraints, and the functions ℓ and p_T define running and terminal costs. We denote $\mathbf{u}(t) = \pi(\mathbf{x}(t); \xi, \nu)$ the control policy we aim to recover. Notably, we assume the distributions of the initial state $\mathbf{x}(0) = \mathbf{x}_0$ and problem parameters $\mathbf{x}_0 \sim P_{\mathbf{x}_0}$ and $\xi \sim P_{\xi}$ to be known, while the dynamics parameterization $\nu \sim P_{\nu}$ may be unknown and require inference from data. After solving (1), the resulting family of policy functions allows for direct adaptation to arbitrary initial states \mathbf{x}_0 , problem parameterizations ξ , and dynamics ν .

3. Zero-Shot Function Encoder-based Differentiable Predictive Control

Function encoders learn compact representations of system dynamics in the form of unique latent coefficients that can be estimated online from data. By conditioning DPC policies on these coef-

1. Code URL will be released in the final version of the paper.

ficients, our approach enables full differentiability while preserving computational efficiency. A diagram detailing our approach is shown in Figure 1, and formalized in Algorithms 1, and 2.

Algorithm 1: Offline learning of FE basis functions for system dynamics	Algorithm 2: Offline learning of parametric neural policies via DPC
Input: set of datasets \mathcal{D} collected from dynamics \mathcal{F} , learning rate α	Input: pre-trained NODE basis functions $\mathbf{g}_1, \dots, \mathbf{g}_B$, learning rate β
1 Initialize basis functions $\mathbf{g}_1, \dots, \mathbf{g}_B$ with trainable parameters $\theta_1, \dots, \theta_B$	1 Initialize policy network $\pi_{\mathbf{W}}$ with trainable parameters \mathbf{W}
2 while <i>not converged</i> do	2 while <i>not converged</i> do
3 for $\mathcal{D}_l \in \mathcal{D}$ do	3 for $\mathbf{x}_0 \sim P_{\mathbf{x}_0}, \xi \sim P_{\xi}, \mathbf{c} \sim P_{\mathbf{c}}$ do
4 reset loss $L = 0$	4 loss $L \leftarrow 0$
5 for $(\mathbf{x}_k, \mathbf{u}_k, \mathbf{x}_{k+1}) \in \mathcal{D}_l$ do	5 for $k = 0, 1, N - 1$ do
6 $\mathbf{c} \leftarrow (\mathbf{G} + \lambda \mathbf{I})^{-1} \mathbf{F}$	6 $\mathbf{u}_k \leftarrow \pi_{\mathbf{W}}(\mathbf{x}_k; \xi, \mathbf{c})$
7 $\hat{\mathbf{x}}_{k+1} \leftarrow \hat{\mathbf{x}}_{k+1}$ from (2)	7 $\mathbf{x}_{k+1} \leftarrow \mathbf{x}_{k+1}$ from (3b)
8 $L \leftarrow L + \ \mathbf{x}_{k+1} - \hat{\mathbf{x}}_{k+1}\ _2^2$	8 end
9 end	9 $L \leftarrow L$ from (3a)
10 $\theta \leftarrow \theta - \alpha \nabla_{\theta} L$	10 $\mathbf{W} \leftarrow \mathbf{W} - \beta \nabla_{\mathbf{W}} L$
11 end	11 end
12 end	12 end
Output: trained basis functions $\mathbf{g}_1, \dots, \mathbf{g}_B$	Output: trained policy network $\pi_{\mathbf{W}}$

3.1. Modeling the Dynamics Using Function Encoders

We model the family of system dynamics using a function encoder (FE) that learns basis functions parameterized by neural ordinary differential equations (NODEs) as in Ingebrand et al. (2024a, 2025). This allows for efficient zero-shot online adaptation in the closed-form.

Offline learning of the FE basis functions. We assume access to a set of datasets \mathcal{D} , consisting of historical trajectories of each $\mathbf{f} \in \mathcal{F}$. More precisely, we have $\mathcal{D} = \{\mathcal{D}_1, \mathcal{D}_2, \dots, \mathcal{D}_r\}$, where each \mathcal{D}_i corresponds to a dynamics function $\mathbf{f}(\cdot, \cdot; \boldsymbol{\nu}_i)$. Each dataset \mathcal{D}_i consists of data in the form of $(\mathbf{x}_k^i, \mathbf{u}_k^i, \mathbf{x}_{k+1}^i)$. This enables data-driven approximation of different dynamics. The FE learns a set of NODE basis functions $\{\mathbf{g}_1, \mathbf{g}_2, \dots, \mathbf{g}_B\}$ that span a subspace $\hat{\mathcal{F}} = \text{span}\{\mathbf{g}_1, \mathbf{g}_2, \dots, \mathbf{g}_B\}$ supported by the data. Given some $\boldsymbol{\nu}$, the dynamics are approximated as $\mathbf{f} \approx \hat{\mathbf{f}} \in \hat{\mathcal{F}}$, which takes the form of a linear combination of the learned basis functions under time discretization,

$$\mathbf{x}_{k+1} = \mathbf{x}_k + \int_{t_k}^{t_{k+1}} \mathbf{f}(\mathbf{x}(t), \mathbf{u}(t); \boldsymbol{\nu}) dt \approx \mathbf{x}_k + \int_{t_k}^{t_{k+1}} \sum_{j=1}^B c_j(\boldsymbol{\nu}) \mathbf{g}_j(\mathbf{x}(t), \mathbf{u}_k; \boldsymbol{\theta}_j) dt, \quad (2)$$

where $\boldsymbol{\theta}_j$ are the network parameters of the basis network \mathbf{g}_j . Importantly, the NODE basis functions $\{\mathbf{g}_1, \mathbf{g}_2, \dots, \mathbf{g}_B\}$ do not depend explicitly on $\boldsymbol{\nu}$; as such, the dynamics function is uniquely determined by the coefficients $\mathbf{c} \in \mathbb{R}^B$. This learning procedure is formalized in Algorithm 1.

Online estimation of FE coefficients. This can be done via regularized least squares optimization. The coefficients \mathbf{c} to some $\mathbf{f} \in \mathcal{F}$ can be computed in closed-form via the normal equation as $(\mathbf{G} + \lambda \mathbf{I})\mathbf{c} = \mathbf{F}$, where $\mathbf{G}_{ij} = \langle \mathbf{g}_i, \mathbf{g}_j \rangle$ and $\mathbf{F}_i = \langle \mathbf{f}, \mathbf{g}_i \rangle$ can both be easily computed using

Monte Carlo integration from a small amount of input-output data collected online. We apply Tikhonov regularization (Golub et al., 1999) in practice to ensure numerical stability. The weights $\{\theta_1, \dots, \theta_B\}$ are frozen during online inference. This representation is key to our approach. By expressing the system in terms of coefficients \mathbf{c} , which we can efficiently compute online, we enable rapid adaptation of the dynamics, thereby making downstream control tasks viable.

Theoretical properties. Function encoders provide a principled approximation for the dynamical model and are theoretically grounded. Prior work in Ingebrand et al. (2025) established that as the number of learned basis functions $B \rightarrow \infty$, the basis functions can span the entire Hilbert space supported by the data. Recent results in Low et al. (2025) strengthen this foundation by formalizing the Hilbert-space structure of the learned representation and by introducing finite-sample guarantees that bound the approximation error once the basis is fixed with an asymptotic rate $\mathcal{O}(\frac{R}{\lambda\sqrt{m}})$, where $\lambda > 0$ is the regularization parameter; m is the number of data points, and R is a constant that depends on the number of basis functions B . These guarantees let us represent new dynamics by estimating only their coefficients without retraining.

3.2. Training the DPC Policy with Function Encoder Dynamics

Differentiable Predictive Control (DPC) (Drgoňa et al., 2022, 2024) is a self-supervised learning method for offline policy optimization that is well suited for solving (1). DPC formulates the pOCP (1) as a differentiable program and trains a neural policy to approximate its closed-loop solution, amortizing the computational cost and eliminating the need for expensive online optimization, while preserving key properties of MPC, such as its model-based formulation, objective function, and constraint handling. Having a known and differentiable parametric dynamical system is a key assumption in the DPC formulation. However, accurately approximating unknown dynamics while preserving the efficient online adaptability of DPC remains an open challenge that we aim to address in this work. We achieve that by leveraging the differentiability and adaptability of FE-NODEs.

DPC with FE-NODE dynamics and neural policies. We combine FE-NODEs with DPC for offline learning of parametric control policies with online zero-shot generalization capability. We use a neural network $\mathbf{u}_k = \pi_{\mathbf{W}}(\mathbf{x}_k; \xi, \mathbf{c}) : \mathbb{R}^{n_x+n_\xi+B} \mapsto \mathbb{R}^{n_u}$ for policy representation with trainable parameters \mathbf{W} . Note that the unknown dynamics parameters ν are replaced with a representation vector \mathbf{c} , consequently we obtain the following training problem in discrete-time form,

$$\min_{\mathbf{W}} \mathbb{E}_{\mathbf{x}_0 \sim P_{\mathbf{x}_0}, \xi \sim P_\xi, \mathbf{c} \sim P_\mathbf{c}} \left[\sum_{k=0}^{N-1} \left(\ell(\mathbf{x}_k, \mathbf{u}_k, \xi) + p(h(\mathbf{x}_k, \xi)) + p(g(\mathbf{u}_k, \xi)) \right) + p_N(\mathbf{x}_N) \right] \quad (3a)$$

$$\text{s.t. } \mathbf{x}_{k+1} = \mathbf{x}_k + \int_{t_k}^{t_{k+1}} \sum_{j=1}^B c_j \mathbf{g}_j(\mathbf{x}(t), \pi_{\mathbf{W}}(\mathbf{x}_k; \xi, \mathbf{c}); \theta_j) dt. \quad (3b)$$

Constraints (1c) are relaxed and incorporated as penalty terms in the objective function (3a). A common choice of penalty functions $p(\cdot)$ for equality constraints is 2-norm $\|\cdot\|_2^2$, while for inequality constraints it is $\|\text{ReLU}(\cdot)\|_2^2$, where ReLU stands for rectifier linear unit function (Glorot et al., 2011). Weights can be used to balance terms in (3a); we omit them here for simplicity of notation.

Offline policy learning. DPC learns parametric control policy by minimizing (3a) in a self-supervised manner. At each update, samples of \mathbf{x}_0 , ξ , and the coefficient vector \mathbf{c} are drawn from

their respective distributions. To evaluate the objective function, full trajectory rollouts are required. The FE-NODE dynamics allow for full differentiability of the computation graph, thereby enabling first-order, gradient-based methods for optimizing the policy network π_W . In practice, automatic differentiation (Baydin et al., 2018) or the adjoint method (Gholami et al., 2019; Zhuang et al., 2020) can be used for gradient computation, depending on the problem specifics. We provide the detailed algorithm for DPC training in Algorithm 2.

Online policy adaptation. By conditioning the DPC policy on FE coefficients, a defining feature of our proposed approach is its zero-shot adaptivity in the policy space, even when the underlying dynamics are not fully known. Once the models are trained during the offline phase, no online model updates are required during evaluation. Only a limited number of observations are needed for dynamics inference and subsequent policy prediction. This makes our approach suitable for fast and accurate transfer of control policies to new and unseen problems. It is also well-suited to scenarios where online system switching may occur and real-time control predictions are required. We provide the outline for online adaptation in Algorithm 3, where we use $\mathbf{x}_{k+1} = \mathbf{x}_k + \Delta t \cdot \mathbf{f}(\mathbf{x}_k, \mathbf{u}_k; \boldsymbol{\nu})$ for simplicity.

Algorithm 3: Online policy adaptation

Input: Trained bases $\{\mathbf{g}_j\}_{j=1}^B$, m online samples $\{\mathbf{x}_k^l, \mathbf{u}_k^l, \mathbf{x}_{k+1}^l\}_{l=1}^m$ for \mathbf{f}
 /* Compute coefficients */
 $\mathbf{G}_{ij} = \frac{1}{m} \sum_{l=1}^m \langle \mathbf{g}_i(\mathbf{x}_k^l, \mathbf{u}_k^l), \mathbf{g}_j(\mathbf{x}_k^l, \mathbf{u}_k^l) \rangle$
 $\mathbf{F}_i = \frac{1}{m} \sum_{l=1}^m \langle (\mathbf{x}_{k+1}^l - \mathbf{x}_k^l) / \Delta t, \mathbf{g}_i(\mathbf{x}_k^l, \mathbf{u}_k^l) \rangle$
 $\mathbf{c} \leftarrow (\mathbf{G} + \lambda \mathbf{I})^{-1} \mathbf{F}$
 /* Evaluate the policy */
 $\mathbf{u}_k \leftarrow \pi_W(\mathbf{x}_k; \boldsymbol{\xi}, \mathbf{c})$
Output: Updated control inputs \mathbf{u}_k

4. Numerical experiments

We conduct extensive numerical experimentation over four examples. These examples arise from various fields in control literature and range in dimensionality and complexity. We demonstrate the accuracy, efficiency, and robustness of our proposed approach. In particular, we highlight the zero-shot generalization capability of our method through experiments involving online dynamics switching, showcasing its advantage over existing approaches.

Implementation details. Function encoder NODE models are configured on a per-example basis with the number of basis functions ranging between 11 and 32, each parameterized by multi-layer perceptrons (MLPs). For all examples, we use 100 data points to compute the function encoder coefficients. For the DPC policy network, a 4-layer MLP with a hidden size of 256 is used for all examples. We use the Adam optimizer (Kingma, 2014) for all examples and train until convergence. We use the RK4 integrator for all systems, with the step size and other hyperparameters selected optimally for each example. We implement MPC using CasADi (Andersson et al., 2019) using the true dynamics as baselines, referred to as the white-box (WB) models in the following sections to compare against our FE-DPC results. All experiments were conducted on a single NVIDIA RTX 5090 GPU. The code is implemented in Pytorch (Paszke et al., 2019) using the NeuroMANCER (Drgoňa et al., 2023) library.

Stabilizing a Van der Pol Oscillator. We first consider the task of stabilizing a nonlinear Van der Pol system, with dynamics $\dot{x}_1 = d \cdot x_2$, $\dot{x}_2 = \mu(1 - x_1^2)x_2 - x_1 + u$, where $[x_1, x_2]^\top \in [-2, 2] \times [-5, 5]$ is the state, $u \in [-3.0, 3.0]$ is the control, and parameters $\mu \sim \mathcal{U}[0.1, 3.0]$ and $d \in \{-1, 1\}$

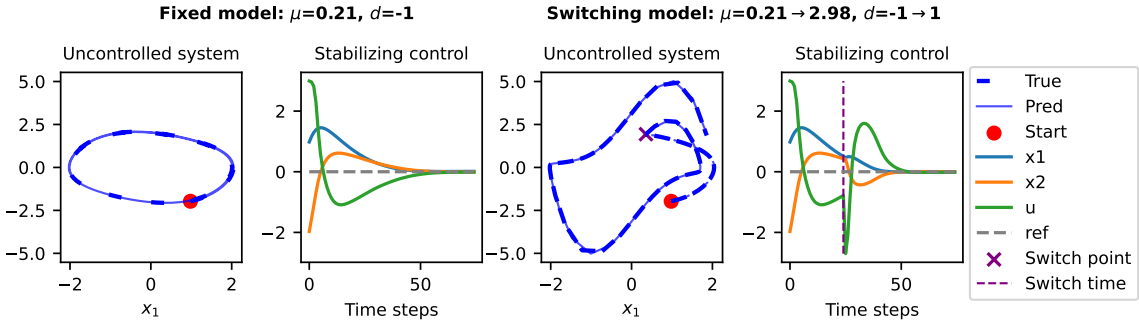


Figure 2: Van der Pol oscillator dynamics under both controlled and uncontrolled scenarios using FE-DPC. **Left:** Uncontrolled and stabilizing results under a fixed dynamics setting. **Right:** Uncontrolled and stabilizing results with changing dynamics; in the example the dynamics switch after 25 steps into the simulation.

determine the dynamics. The objective is to “stabilize” the system, that is, $p_N(\mathbf{x}_N) = \|\mathbf{x}_N\|^2$ and $\ell(\mathbf{x}_k, \mathbf{u}_k, \xi) = \|\mathbf{u}_k\|^2$ in eq. (3a).

Predictions from the learned function encoder and control policies from DPC are shown in Figure 2. The first two plots illustrate system behavior, without and with control, respectively, under fixed unknown dynamics that are identified in a zero-shot manner using least-squares estimation from measurement data. In the uncontrolled case, the predicted trajectories closely match the true trajectories simulated using the white-box model, validating the accuracy of the identified surrogate dynamics. The system is successfully stabilized within the prescribed input and state bounds when learned DPC policies are applied. The next two plots depict a scenario where the system parameters are switched during simulation. Despite an abrupt model switch, the proposed solution adapts online to stabilize the system. Importantly, this adaptation requires no retraining as the learned model is robust to parametric variations.

Reference Tracking of a Two-tank System. We consider level regulation of a two-tank system given the dynamics $\dot{x}_1 = d_1(1-v)p - d_2\sqrt{x_1}$, $\dot{x}_2 = d_1vp + d_2\sqrt{x_1} - d_2\sqrt{x_2}$, where $[x_1, x_2]^\top \in [0, 1]^2$ are the tank liquid levels, and control inputs $[p, v]^\top \in [0, 1]^2$ correspond to pump modulation and valve opening, respectively. The system is parameterized by inlet and outlet valve coefficients d_1 and d_2 , with $d_1 \sim \mathcal{U}[0.06, 0.1]$ and $d_2 \sim \mathcal{U}[0.01, 0.06]$. The objective is to regulate the tank levels under different system parameterization to track desired reference values through coordinated

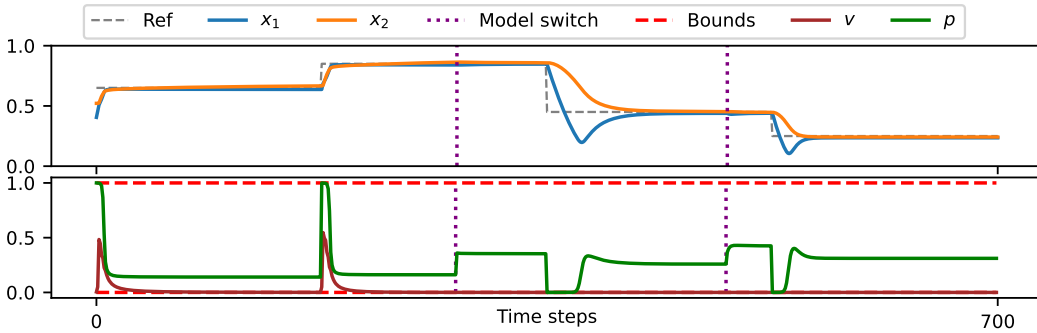


Figure 3: Two-tank system reference tracking under multiple system switches using FE-DPC.

modulation of the pump and valve control inputs. We have $p_N(\mathbf{x}_N) = \|\mathbf{x}_N - \mathbf{x}_{\text{ref}}(\xi)\|^2$ and $\ell(\mathbf{x}_k, \mathbf{u}_k, \xi) = \|\mathbf{x}_k - \mathbf{x}_{\text{ref}}(\xi)\|^2 + \|\mathbf{u}_k\|^2$ in training where $\mathbf{x}_{\text{ref}}(\xi)$ can vary.

Figure 3 demonstrates accurate and stable reference tracking as both the system parameters and reference trajectories vary at inference time. The simulation spans 700 time steps, during which the predicted and reference trajectories remain closely aligned, highlighting the accuracy of the learned dynamics model. The controller maintains consistent tracking performance through multiple system switches, showing strong robustness to changing conditions. Moreover, constraints on the control variable remain satisfied throughout the simulation.

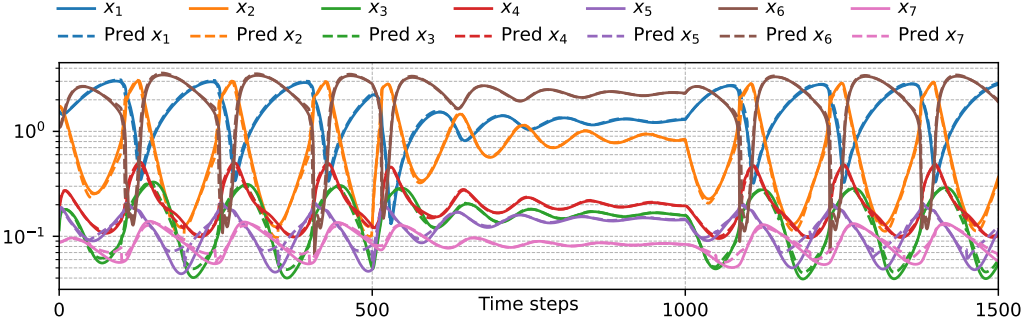


Figure 4: True and predicted uncontrolled GO system dynamics. System parameterizations change every 500 time steps, and predictions are calibrated against the true states every 50 steps.

Reference Tracking of a Glycolytic Oscillator (GO). We consider a highly nonlinear and stiff ODE system (Daniels and Nemenman, 2015), which models the yeast glycolysis dynamics as:

$$\begin{cases} \dot{x}_1 = J_0 - \frac{k_1 x_1 x_6}{1+(x_6/K_1)^q} + u, \\ \dot{x}_2 = 2\frac{k_1 x_1 x_6}{1+(x_6/K_1)^q} - k_2 x_2 (N - x_5) - k_6 x_2 x_5, \\ \dot{x}_3 = k_2 x_2 (N - x_5) - k_3 x_3 (A - x_6), \\ \dot{x}_4 = k_3 x_3 (A - x_6) - k_4 x_4 x_5 - \kappa (x_4 - x_7), \\ \dot{x}_5 = k_2 x_2 (N - x_5) - k_4 x_4 x_5 - k_6 x_2 x_5, \\ \dot{x}_6 = -2\frac{k_1 x_1 x_6}{1+(x_6/K_1)^q} + 2k_3 x_3 (A - x_6) - k_5 x_6, \\ \dot{x}_7 = \psi \kappa (x_4 - x_7) - k x_7. \end{cases} \quad (4)$$

where $[x_1, \dots, x_7] \sim \mathcal{U}([0.15, 0.19, 0.04, 0.10, 0.08, 0.14, 0.05], [1.60, 2.16, 0.20, 0.35, 0.30, 2.67, 0.10])$ represent concentrations of the seven biochemical species as states. We define control input $u \in [-4, 4]$. For system parameterization, we set $J_0 = 2.5$, $k_2 = 6$, $k_3 = 16$, $k_4 = 100$, $k_5 = 1.28$, $k_6 = 12$, $q = 4$, $N = 1$, $A = 4$, $\kappa = 13$, $\psi = 0.1$, and $k = 1.8$ to be fixed, and $k_1 \in \{80, 90, 100\}$ and $K_1 \in \{0.5, 0.75\}$ uniquely define each dynamics model. The system in Eq. (4) exhibits stiff behavior, requiring smaller integration steps and, consequently, a longer prediction horizon for control. Combined with its relatively high dimensionality, this makes the problem particularly challenging. Prediction horizon for FE-DPC and baseline WB-MPC is set to be 50. In Figure 4, the uncontrolled evolution of the dynamical system under different parameterizations of k_1 and K_1 is shown to alternate between stationary and oscillatory behavior. Evidently, the FE-NODE approximation achieves high accuracy under the prediction horizon.

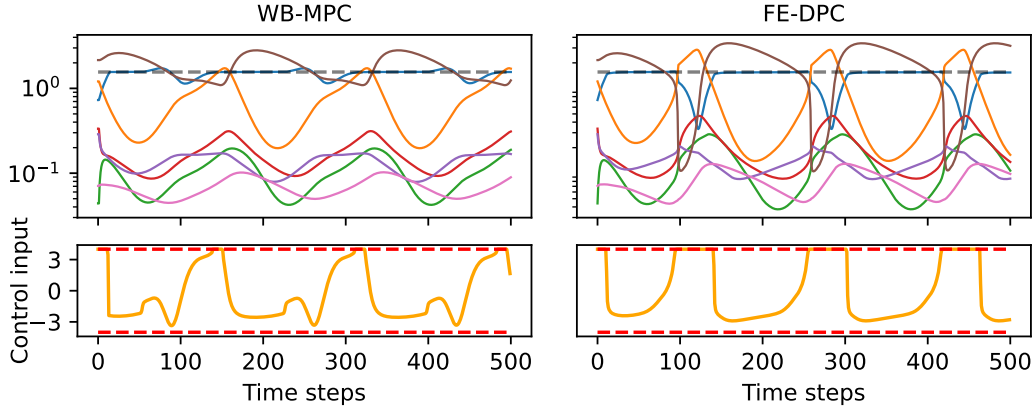


Figure 5: WB-MPC (left) and FE-DPC (right) based reference tracking of x_1 (blue) state.

For control, only the first state x_1 is directly actuated by the control input u , and it also serves as the reference-tracking state, while the remaining 6 states evolve freely according to the nonlinear dynamics. The control objective is defined by $p_N(\mathbf{x}_N) = \|\mathbf{x}_N - \mathbf{x}_{\text{ref}}(\boldsymbol{\xi})\|^2$ and $\ell(\mathbf{x}_k, \mathbf{u}_k, \boldsymbol{\xi}) = \|\mathbf{x}_k - \mathbf{x}_{\text{ref}}(\boldsymbol{\xi})\|^2 + \|\mathbf{u}_k\|^2$ in eq. (3a). Figure 5 compares the performance of the controlled GO systems between the MPC solution under the known white-box system dynamics and the FE-DPC model prediction under online system identification. In both cases, the control input saturates within bounds, and the controlled state exhibits an offset from the reference. WB-MPC solution achieves a lower tracking error since it optimizes under known system dynamics, while FE-DPC predicts a simpler plan that nonetheless accurately tracks the reference until the control saturates. As we show in Table 1, computational efficiency is one of the main advantages of FE-DPC.

Controlling a Quadrotor. We consider a quadrotor flight control based on a 12-dimensional nonlinear dynamic model (Beard, 2008; Lopez et al., 2022) that captures the vehicle’s translational and rotational motion under thrust and torque inputs. The states include position, attitude, and velocity variables, while the 3-dimensional control inputs correspond to the total thrust and roll/pitch torques. System parameters such as mass and moments of inertia are randomly sampled and uniquely define the vehicle’s motion. The control objective is to stabilize the vehicle at a target altitude of 0.4m while having near-zero linear and angular velocities, we impose no running cost for the example. The high dimensionality and nonlinearity of the dynamics make the problem particularly challenging. We include a detailed problem definition in Appendix A.

Figure 6 demonstrates the generalization capability of FE-DPC. The policy is evaluated on 20 distinct system parameterizations, each initialized randomly within state bounds. To test robustness, each system undergoes an abrupt parameter switch at a random time between 2 and 20 seconds. In all cases, the controller maintains hover within the terminal cost tolerance $p_N(\mathbf{x}_N)$, indicating the learned parametric policies are robust to system changes under even complex dynamics.

Inference-time comparisons. One of the main advantages of our approach lies in its computational efficiency. Computation times measured during validation are presented in Table 1. Since baseline MPC cannot accommodate adaptive scenarios, we restrict this comparison to single parameter cases. MPC solvers can be slow due to the need for extensive online computation. At inference time, our method achieves a speed-up between 2.3 and 71.5 times over its MPC counterpart across the tested examples. The tracking error is evaluated using the mean squared loss (MSE) between predicted and reference states. While MPC attains the lowest tracking error due

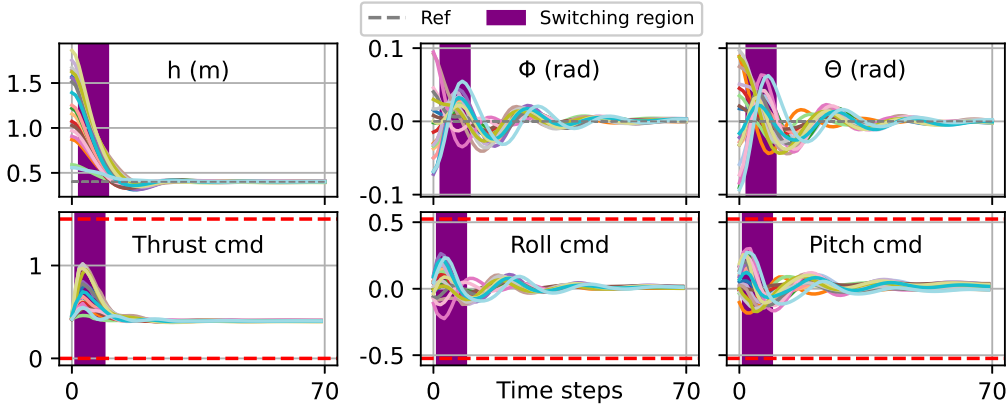


Figure 6: 20 quadrotor models with distinct dynamics parameterization are randomly initialized within state bounds. Each experiences a random dynamics switch between 2-20 s. FE-DPC successfully stabilizes all models at the reference height of $h = 0.4\text{m}$.

to its access to exact system dynamics, FE-DPC delivers comparable accuracy across all examples despite relying on learned system identification and control approximations. The ablation study in [Ingebrand et al. \(2025\)](#) suggests that increasing B can lead to better model accuracy, at the cost of computational efficiency. Additionally, [Low et al. \(2025\)](#) introduces the use of PCA to derive a compact representation of the dynamics space, a technique we aim to incorporate in future work.

Algorithm	Metric	Van der Pol	Two Tank	GO	Quadrotor
FE-DPC	Error (MSE)	0.002683	0.008452	0.180299	0.022003
	Time (s)	0.53	1.13	5.89	1.93
WB-MPC	Error (MSE)	0.002653	0.004164	0.032320	0.024208
	Time (s)	1.21	6.75	136.07	155.85

Table 1: Comparison of error (MSE) and computation time (s) for each benchmark.

5. Conclusion

In this work, we present an end-to-end pipeline that combines function encoder-based system identification and differential predictive control to solve parametric optimal control problems. Our approach allows for zero-shot generalization of system approximations of varying and unknown dynamics, given limited observations, and predicts corresponding policies. It is well-suited for problems requiring repeated online evaluation and enables real-time policy adaptation in response to system changes during inference. We validate the efficiency and accuracy of our approach through extensive numerical experiments. While the proposed framework demonstrates strong empirical performance across a range of nonlinear and high-dimensional control problems, some limitations remain. Given the data-driven nature of the FE-NODE training, sufficient data to represent the space of possible system dynamics is necessary for ensuring performance. We also note that while we focus only on MLPs in this work, this choice of parameterization may face difficulty when dealing with problems exhibiting high stiffness or requiring accurate predictions over longer temporal horizons. Additional design choices, such as ([Kim et al., 2021](#); [Linot et al., 2023](#)) may be explored; however, we will leave this for future work.

Acknowledgments

Hassan Iqbal, Xingjian Li, and Krishna Kumar were partially funded by NSF 2339678 and 2321040. Ján Drgoňa was supported by the Ralph O'Connor Sustainable Energy Institute at Johns Hopkins University. Tyler Ingebrand, Adam Thorpe, and Ufuk Topcu are supported in part by DARPA HR0011-24-9-0431 and NSF 2214939. Any opinions, findings, conclusions or recommendations expressed in this material are those of the authors and do not necessarily reflect the views of the funding organizations.

References

Emre Adabag, Miloni Atal, William Gerard, and Brian Plancher. Mpcgpu: Real-time nonlinear model predictive control through preconditioned conjugate gradient on the gpu. In *2024 IEEE International Conference on Robotics and Automation (ICRA)*, pages 9787–9794. IEEE, 2024.

R.K. Al Seyab and Y. Cao. Nonlinear system identification for predictive control using continuous time recurrent neural networks and automatic differentiation. *Journal of Process Control*, 18(6): 568–581, 2008. ISSN 0959-1524. doi: <https://doi.org/10.1016/j.jprocont.2007.10.012>.

Joel A E Andersson, Joris Gillis, Greg Horn, James B Rawlings, and Moritz Diehl. CasADI – A software framework for nonlinear optimization and optimal control. *Mathematical Programming Computation*, 11(1):1–36, 2019. doi: 10.1007/s12532-018-0139-4.

Atilim Gunes Baydin, Barak A Pearlmutter, Alexey Andreyevich Radul, and Jeffrey Mark Siskind. Automatic differentiation in machine learning: a survey. *Journal of machine learning research*, 18(153):1–43, 2018.

Randal W Beard. Quadrotor dynamics and control. *Brigham Young University*, 19(3):46–56, 2008.

Vladimir Beliaev, Nadezhda Kunicina, Anastasija Ziravecka, Martins Bisenieks, Roberts Grants, and Antons Patlins. Development of adaptive control system for aerial vehicles. *Applied Sciences*, 13(23):12940, 2023.

Julian Berberich, Johannes Köhler, Matthias A. Müller, and Frank Allgöwer. Data-driven model predictive control with stability and robustness guarantees. *IEEE Transactions on Automatic Control*, 66(4):1702–1717, 2021. doi: 10.1109/TAC.2020.3000182.

Francesco Borrelli, Alberto Bemporad, and Manfred Morari. *Predictive Control for Linear and Hybrid Systems*. Cambridge University Press, USA, 1st edition, 2017. ISBN 1107652871.

Steven L Brunton, Joshua L Proctor, and J Nathan Kutz. Discovering governing equations from data by sparse identification of nonlinear dynamical systems. *Proceedings of the national academy of sciences*, 113(15):3932–3937, 2016.

Ricky TQ Chen, Yulia Rubanova, Jesse Bettencourt, and David K Duvenaud. Neural ordinary differential equations. *Advances in neural information processing systems*, 31, 2018a.

Steven Chen, Kelsey Saulnier, Nikolay Atanasov, Daniel D Lee, Vijay Kumar, George J Pappas, and Manfred Morari. Approximating explicit model predictive control using constrained neural networks. In *2018 Annual American control conference (ACC)*, pages 1520–1527. IEEE, 2018b.

Bryan C Daniels and Ilya Nemenman. Efficient inference of parsimonious phenomenological models of cellular dynamics using s-systems and alternating regression. *PLoS one*, 10(3):e0119821, 2015.

Ján Drgoňa, Karol Kiš, Aaron Tuor, Draguna Vrabie, and Martin Klaučo. Differentiable predictive control: Deep learning alternative to explicit model predictive control for unknown nonlinear systems. *Journal of Process Control*, 116:80–92, 2022.

Ján Drgoňa, Aaron Tuor, James Koch, Madelyn Shapiro, Bruno Jacob, and Draguna Vrabie. Neuro-MANCER: Neural Modules with Adaptive Nonlinear Constraints and Efficient Regularizations. 2023. URL <https://github.com/pnnl/neuromancer>.

Ján Drgoňa, Aaron Tuor, and Draguna Vrabie. Learning constrained parametric differentiable predictive control policies with guarantees. *IEEE Transactions on Systems, Man, and Cybernetics: Systems*, 54(6):3596–3607, 2024.

Urban Fasel, Eurika Kaiser, J Nathan Kutz, Bingni W Brunton, and Steven L Brunton. Sindy with control: A tutorial. In *2021 60th IEEE conference on decision and control (CDC)*, pages 16–21. IEEE, 2021.

Gianluca Frison and Moritz Diehl. HPIPM: a high-performance quadratic programming framework for model predictive control. *IFAC-PapersOnLine*, 53(2):6563–6569, 2020.

Amir Gholami, Kurt Keutzer, and George Biros. Anode: Unconditionally accurate memory-efficient gradients for neural odes. *arXiv preprint arXiv:1902.10298*, 2019.

Xavier Glorot, Antoine Bordes, and Yoshua Bengio. Deep sparse rectifier neural networks. In *Proceedings of the fourteenth international conference on artificial intelligence and statistics*, pages 315–323. JMLR Workshop and Conference Proceedings, 2011.

Gene H Golub, Per Christian Hansen, and Dianne P O’Leary. Tikhonov regularization and total least squares. *SIAM Journal on Matrix Analysis and Applications*, 21(1):185–194, 1999.

Michael Hertneck, Johannes Köhler, Sebastian Trimpe, and Frank Allgöwer. Learning an approximate model predictive controller with guarantees. *IEEE Control Systems Letters*, 2(3):543–548, 2018.

Lukas Hewing, Kim P Wabersich, Marcel Menner, and Melanie N Zeilinger. Learning-based model predictive control: Toward safe learning in control. *Annual Review of Control, Robotics, and Autonomous Systems*, 3(1):269–296, 2020.

Boris Houska, Hans Joachim Ferreau, and Moritz Diehl. Acado toolkit—an open-source framework for automatic control and dynamic optimization. *Optimal control applications and methods*, 32(3):298–312, 2011.

Tyler Ingebrand, Adam Thorpe, and Ufuk Topcu. Zero-shot transfer of neural odes. *Advances in Neural Information Processing Systems*, 37:67604–67626, 2024a.

Tyler Ingebrand, Amy Zhang, and Ufuk Topcu. Zero-shot reinforcement learning via function encoders. In *International Conference on Machine Learning*, pages 21007–21019. PMLR, 2024b.

Tyler Ingebrand, Adam J Thorpe, and Ufuk Topcu. Function encoders: A principled approach to transfer learning in hilbert spaces. *arXiv preprint arXiv:2501.18373*, 2025.

Rolf Isermann and Marco Münchhof. *Identification of dynamic systems: an introduction with applications*, volume 85. Springer, 2011.

Zhong-Ping Jiang, Tao Bian, Weinan Gao, et al. Learning-based control: A tutorial and some recent results. *Foundations and Trends® in Systems and Control*, 8(3):176–284, 2020.

Wanxin Jin, Zhaoran Wang, Zhuoran Yang, and Shaoshuai Mou. Pontryagin differentiable programming: An end-to-end learning and control framework. *Advances in Neural Information Processing Systems*, 33:7979–7992, 2020.

Benjamin Karg and Sergio Lucia. Efficient representation and approximation of model predictive control laws via deep learning. *IEEE transactions on cybernetics*, 50(9):3866–3878, 2020.

Suyong Kim, Weiqi Ji, Sili Deng, Yingbo Ma, and Christopher Rackauckas. Stiff neural ordinary differential equations. *Chaos: An Interdisciplinary Journal of Nonlinear Science*, 31(9), 2021.

Diederik P Kingma. Adam: A method for stochastic optimization. *arXiv preprint arXiv:1412.6980*, 2014.

Stefan Klus, Feliks Nüske, Sebastian Peitz, Jan-Hendrik Niemann, Cecilia Clementi, and Christof Schütte. Data-driven approximation of the koopman generator: Model reduction, system identification, and control. *Physica D: Nonlinear Phenomena*, 406:132416, 2020.

Torsten Koller, Felix Berkenkamp, Matteo Turchetta, and Andreas Krause. Learning-based model predictive control for safe exploration. In *2018 IEEE conference on decision and control (CDC)*, pages 6059–6066. IEEE, 2018.

Milan Korda and Igor Mezić. On convergence of extended dynamic mode decomposition to the Koopman operator. *Journal of Nonlinear Science*, 28(2):687–710, 2018.

Quentin Le Lidec, Wilson Jallet, Louis Montaut, Ivan Laptev, Cordelia Schmid, and Justin Carpentier. Contact models in robotics: a comparative analysis. *IEEE Transactions on Robotics*, 2024.

Peilun Li, Kaiyuan Tan, and Thomas Beckers. Napi-mpc: Neural accelerated physics-informed mpc for nonlinear pde systems. In *Proceedings of the 7th Annual Learning for Dynamics & Control Conference*, volume 283 of *Proceedings of Machine Learning Research*, pages 1230–1242. PMLR, 04–06 Jun 2025a.

Xingjian Li, Kelvin Kan, Deepanshu Verma, Krishna Kumar, Stanley Osher, and Ján Drgoňa. Zero-shot transferable solution method for parametric optimal control problems. *arXiv preprint arXiv:2509.18404*, 2025b.

Alec J Linot, Joshua W Burby, Qi Tang, Prasanna Balaprakash, Michael D Graham, and Romit Maulik. Stabilized neural ordinary differential equations for long-time forecasting of dynamical systems. *Journal of Computational Physics*, 474:111838, 2023.

Bjoern List, Li-Wei Chen, Kartik Bali, and Nils Thuerey. Differentiability in unrolled training of neural physics simulators on transient dynamics. *Computer Methods in Applied Mechanics and Engineering*, 433:117441, 2025.

Diego Manzanas Lopez, Matthias Althoff, Luis Benet, Xin Chen, Jiameng Fan, Marcelo Forets, Chao Huang, Taylor T Johnson, Tobias Ladner, Wenchao Li, et al. Arch-comp22 category report: Artificial intelligence and neural network control systems (ainnncs) for continuous and hybrid systems plants. In *9th International Workshop on Applied Verification of Continuous and Hybrid Systems (ARCH22)*, pages 142–184. EasyChair, 2022.

Su Ann Low, Quentin Rommel, Kevin S Miller, Adam J Thorpe, and Ufuk Topcu. Function spaces without kernels: Learning compact hilbert space representations. *arXiv preprint arXiv:2509.20605*, 2025.

Andreas B Martinsen, Anastasios M Lekkas, and Sébastien Gros. Combining system identification with reinforcement learning-based mpc. *IFAC-PapersOnLine*, 53(2):8130–8135, 2020.

Derek Onken, Levon Nurbekyan, Xingjian Li, Samy Wu Fung, Stanley Osher, and Lars Ruthotto. A neural network approach for high-dimensional optimal control applied to multiagent path finding. *IEEE Transactions on Control Systems Technology*, 31(1):235–251, 2022.

Ivana Palunko and Rafael Fierro. Adaptive control of a quadrotor with dynamic changes in the center of gravity. *IFAC Proceedings Volumes*, 44(1):2626–2631, 2011.

Adam Paszke, Sam Gross, Francisco Massa, Adam Lerer, James Bradbury, Gregory Chanan, Trevor Killeen, Zeming Lin, Natalia Gimelshein, Luca Antiga, et al. Pytorch: An imperative style, high-performance deep learning library. *Advances in neural information processing systems*, 32, 2019.

G. Pin, M. Filippo, F.A. Pellegrino, G. Fenu, and T. Parisini. Approximate model predictive control laws for constrained nonlinear discrete-time systems: analysis and offline design. *International Journal of Control*, 86(5):804–820, 2013. doi: 10.1080/00207179.2012.762121.

Rik Pintelon and Johan Schoukens. *System identification: a frequency domain approach*. John Wiley & Sons, 2012.

Aowabin Rahman, Ján Drgoňa, Aaron Tuor, and Jan Strube. Neural ordinary differential equations for nonlinear system identification. In *2022 American control conference (ACC)*, pages 3979–3984. IEEE, 2022.

James Blake Rawlings, David Q Mayne, Moritz Diehl, et al. *Model predictive control: theory, computation, and design*, volume 2. Nob Hill Publishing Madison, WI, 2020.

Tariq Samad, Margret Bauer, Scott Bortoff, Stefano Di Cairano, Lorenzo Fagiano, Peter Fogh Odgaard, R Russell Rhinehart, Ricardo Sánchez-Peña, Atanas Serbezov, Finn Ankersen, et al. Industry engagement with control research: Perspective and messages. *Annual Reviews in Control*, 49:1–14, 2020.

Max Schwenzer, Muzaffer Ay, Thomas Bergs, and Dirk Abel. Review on model predictive control: An engineering perspective. *The International Journal of Advanced Manufacturing Technology*, 117(5):1327–1349, 2021.

Robin Verschueren, Gianluca Frison, Dimitris Kouzoupis, Jonathan Frey, Niels van Duijkeren, Andrea Zanelli, Branimir Novoselnik, Thivaharan Albin, Rien Quirynen, and Moritz Diehl. *acados – a modular open-source framework for fast embedded optimal control.* *Mathematical Programming Computation*, 2021.

William Ward, Sarah Etter, Jesse Quattrociocchi, Christian Ellis, Adam J Thorpe, and Ufuk Topcu. Zero to autonomy in real-time: Online adaptation of dynamics in unstructured environments. *arXiv preprint arXiv:2509.12516*, 2025.

Liang Wu and Alberto Bemporad. A Simple and Fast Coordinate-Descent Augmented-Lagrangian Solver for Model Predictive control. *IEEE Transactions on Automatic Control*, 68(11):6860–6866, 2023.

Andrea Zanelli, Alexander Domahidi, Juan Jerez, and Manfred Morari. FORCES NLP: an efficient implementation of interior-point methods for multistage nonlinear nonconvex programs. *International Journal of Control*, 93(1):13–29, 2020.

Juntang Zhuang, Nicha Dvornek, Xiaoxiao Li, Sekhar Tatikonda, Xenophon Papademetris, and James Duncan. Adaptive checkpoint adjoint method for gradient estimation in neural ode. In *International Conference on Machine Learning*, pages 11639–11649. PMLR, 2020.

Appendix A. Supplementary Materials

In this section, we provide additional details on the Quadrotor control example, including the full dynamics model and corresponding control objectives.

Controlling a quadrotor

We use the quadrotor dynamics (Beard, 2008; Lopez et al., 2022) described by system of ODEs as,

$$\left\{ \begin{array}{l} \dot{p}_n = \cos \theta \cos \psi u + (\sin \phi \sin \theta \cos \psi - \cos \phi \sin \psi) v + (\cos \phi \sin \theta \cos \psi + \sin \phi \sin \psi) w, \\ \dot{p}_e = \cos \theta \sin \psi u + (\sin \phi \sin \theta \sin \psi + \cos \phi \cos \psi) v + (\cos \phi \sin \theta \sin \psi - \sin \phi \cos \psi) w, \\ \dot{h} = \sin \theta u - \sin \phi \cos \theta v - \cos \phi \cos \theta w, \\ \dot{u} = rv - qw - g \sin \theta, \\ \dot{v} = pw - ru + g \cos \theta \sin \phi, \\ \dot{w} = qu - pv + g \cos \theta \cos \phi - F/m, \\ \dot{\phi} = p + \sin \phi \tan \theta q + \cos \phi \tan \theta r, \\ \dot{\theta} = \cos \phi q - \sin \phi r, \\ \dot{\psi} = (\sin \phi / \cos \theta) q + (\cos \phi / \cos \theta) r, \\ \dot{p} = ((J_y - J_z) / J_x) qr + (1 / J_x) \tau_\phi, \\ \dot{q} = ((J_z - J_x) / J_y) pr + (1 / J_y) \tau_\theta, \\ \dot{r} = ((J_x - J_y) / J_z) pq + (1 / J_z) \tau_\psi. \end{array} \right.$$

where p_n, p_e, h denote the inertial positions (north, east, altitude), u, v, w are the body-frame linear velocities, p, q, r are the body angular rates, and ϕ, θ, ψ are the roll, pitch, and yaw Euler angles. The total thrust is F , and $\tau_\phi, \tau_\theta, \tau_\psi$ are the control torques about the body axes. Here, we make standard assumptions as in other works where $g = 9.81$ and $\tau_\psi = 0$. The control inputs α enter the system via,

$$\begin{aligned} F &= mg - 10(h - \alpha_1) + 3w, \\ \tau_\phi &= -(\phi - \alpha_2) - p, \\ \tau_\theta &= -(\theta - \alpha_3) - q. \end{aligned}$$

The control inputs are sampled as,

$$[\alpha_1, \alpha_2, \alpha_3]^\top \in [\alpha_{\min}, \alpha_{\max}] = \begin{bmatrix} 0, -0.524, -0.524 \\ 1.5, 0.524, 0.524 \end{bmatrix}^\top \subset \mathbb{R}^3.$$

The system parameters are sampled as follows,

$$m \sim \mathcal{U}[1.2, 1.6], \quad J_x = J_y \sim \mathcal{U}[0.050, 0.058], \quad J_z \sim \mathcal{U}[0.090, 0.110].$$

The objective is for the quadrotor to maintain an altitude of 0.4 with zero linear and angular velocities. This setting provides a challenging benchmark due to the strong coupling and nonlinearity in the dynamics, making it a suitable test case for evaluating the proposed FE-DPC framework.